

# Spectral-Aligned Pruning for Universal Error-Correcting Code Transformers

Sanghyeon Cho<sup>1</sup> Taewoo Park<sup>1</sup> Seong-Joon Park<sup>2</sup> Dae-Young Yun<sup>3</sup> Hee-Youl Kwak<sup>3</sup> Sang-Hyo Kim<sup>4</sup>  
Yongjune Kim<sup>1</sup>

## Abstract

Recently, the Foundation Error Correction Code Transformer (FECCT) has emerged as a promising *universal* channel decoder, achieving competitive decoding performance across diverse code families by relying on a single shared model backbone, optionally followed by code-specific retraining. Despite this flexibility, the high computational complexity and large parameter footprint of transformer-based decoders present substantial obstacles to practical deployment. To address these challenges, we investigate structured pruning for FECCT and propose Spectral-Aligned Pruning (SAP), a structure-aware framework that enables cross-code reuse of structured pruning masks across codes by leveraging the spectrum of the corresponding bipartite graph. After pruning, SAP performs per-code recovery via parameter-efficient low-rank adaptation (LoRA), enabling a shared pruned backbone while storing only small code-specific adapter parameters. Experiments across diverse codes show that SAP achieves decoding performance comparable to dedicated per-code pruning, while enabling substantial reductions in computational cost and model memory footprint through kernel-level structured pruning.

## 1. Introduction

Error-Correcting Codes (ECCs) are fundamental to reliable digital communication, enabling accurate recov-

<sup>1</sup>Department of Electrical Engineering, Pohang University of Science and Technology (POSTECH), Pohang 37673, South Korea

<sup>2</sup>Institute of Artificial Intelligence, Pohang University of Science and Technology (POSTECH), Pohang 37673, South Korea

<sup>3</sup>Department of Electrical, Electronic and Computer Engineering, University of Ulsan, Ulsan 44610, South Korea

<sup>4</sup>Department of Electrical and Computer Engineering, Sungkyunkwan University, Suwon 16419, South Korea. Correspondence to: Yongjune Kim <yongjune@postech.ac.kr>.

*Proceedings of the 43<sup>rd</sup> International Conference on Machine Learning*, Seoul, South Korea. PMLR 306, 2026. Copyright 2026 by the author(s).

ery of information over noisy channels. Over decades, coding theory has developed well-established code families and decoding algorithms by exploiting algebraic and graphical structures (MacWilliams & Sloane, 1977; Richardson & Urbanke, 2008). Each code family is usually accompanied by decoding algorithms that are optimized for its specific algebraic or graphical structure.

Transformers have demonstrated that self-attention can effectively model long-range dependencies through flexible token interactions (Vaswani et al., 2017). This capability has motivated neural ECC decoders such as the Error Correction Code Transformer (ECCT) (Choukroun & Wolf, 2022), which incorporates bipartite graph structure into the decoding process through code-aware attention. ECCT enables a single decoding *algorithm* to operate across multiple code families; however, the resulting model architecture—and thus the number of parameters—depends on the code length and rate. The Foundation Error Correction Code Transformer (FECCT) extends this direction by unifying not only the decoding algorithm but also the model *architecture and parameter set* (Choukroun & Wolf, 2024). In particular, FECCT uses a single decoder architecture with a fixed parameter set shared across different code families and code parameters, while allowing the parameter values to be retrained for individual codes.

Despite these advances, transformer-based decoders remain expensive in terms of computational cost and model memory footprint, limiting their practicality in resource-constrained receivers. To mitigate the computational and memory overheads of transformer-based ECC decoders, several approaches have been explored. Architectural approaches, such as Cross-Attention Message-Passing Transformer (CrossMPT), redesign the attention mechanism to improve efficiency (Park et al., 2025). In addition, quantization-based approaches have been proposed, including Accelerating Error Correction Code Transformers (AECCT), which adopt ternary weight quantization (Levy et al., 2024). However, structured pruning for transformer-based ECC decoders has not been systematically studied.

In this paper, we investigate *structured pruning* for universal transformer-based decoders. In transformer architec-

tures, structured pruning removes attention heads and feed-forward network (FFN) channels, yielding practical kernel-level speedups (Michel et al., 2019; Voita et al., 2019). A pruning mask specifies which structural units (e.g., attention heads and FFN channels) are retained or removed, and is typically derived from importance scores computed on a calibration set, incurring significant computational overhead (Zafir et al., 2021; Kwon et al., 2022; Cheng et al., 2024). In the context of ECC decoders, it is important to determine pruning masks that preserve decoding performance. A straightforward approach is to derive a separate pruning mask for each code; however, this becomes impractical for universal decoders that must support a large and diverse set of codes. To address this limitation, we aim to reuse pruning masks across different codes, thereby reducing the cost of searching for pruning masks. This naturally raises a key question:

*When can structured pruning masks be shared across different codes while maintaining decoding performance?*

However, directly comparing codes is challenging due to their varying block lengths and rates. Consequently, efficient mask reuse requires a framework that can quantify structural similarity across heterogeneous codes.

To answer this question, we propose *Spectral-Aligned Pruning (SAP)*, a structure-aware framework that provides a principled criterion for reusing structured pruning masks across different codes. SAP enables cross-code reuse of structured pruning masks by aligning codes according to the spectrum of their bipartite graphs. Given a target code, SAP computes the spectrum of its adjacency matrix and retrieves the nearest entry from a pruning mask library using a spectral distance. If the spectral similarity score to the nearest neighbor exceeds a predefined threshold, SAP reuses the associated mask to prune FECCT for the target code. Otherwise, SAP derives a new structured pruning mask using code-conditioned importance estimation and updates the library by inserting the resulting spectral signature and pruning mask pair. By using spectral proximity as the reuse criterion and expanding the library only when necessary, SAP amortizes the pruning mask search cost while avoiding unreliable sharing across structurally dissimilar bipartite graphs.

To efficiently recover decoding performance after pruning, we adopt a lightweight and parameter-efficient recovery step using *low-rank adaptation (LoRA)* adapters on top of the pruned backbone. We freeze the parameters of the pruned backbone and fine-tune only the code-specific rank-decomposition matrices. This design enables storage-efficient multi-code deployment by sharing a pruned backbone while storing only a small set of LoRA parameters for each code, substantially reducing storage overhead compared to full fine-tuned models.

## Contributions.

- **(C1)** We formulate and apply a principled *structured* pruning for transformer-based ECC decoders, instantiated on the universal FECCT backbone, enabling reductions in computational cost and model memory footprint.
- **(C2)** We identify a strong correlation between the spectral similarity of bipartite graphs and cross-code pruning mask overlap. Leveraging this observation, we propose *Spectral-Aligned Pruning (SAP)*, a framework that enables efficient mask reuse via lightweight library retrieval, threshold-based reuse decisions, and on-demand library expansion.
- **(C3)** To efficiently recover decoding performance after structured pruning, we introduce a parameter-efficient retraining strategy based on LoRA, whereas prior approaches such as FECCT typically recover decoding performance by retraining the full set of model parameters. To the best of our knowledge, this is the first application of LoRA for post-pruning recovery in transformer-based ECC decoders.
- **(C4)** Across multiple code families and code parameters, SAP achieves decoding performance comparable to dedicated per-code pruning after recovery and yields substantial reductions in computational cost and model memory footprint through structured pruning.

## 2. Background

### 2.1. Error-Correcting Codes

We consider an  $(n, k)$  binary linear block code with rate  $k/n$ . A code is specified by a generator matrix  $G \in \{0, 1\}^{k \times n}$  and a parity-check matrix  $H \in \{0, 1\}^{(n-k) \times n}$  satisfying  $GH^\top = 0$  over GF(2). Encoding maps a message  $m \in \{0, 1\}^k$  to a codeword  $x = mG \in \{0, 1\}^n$  such that  $Hx^\top = 0$  over GF(2). We adopt the standard binary phase-shift keying (BPSK) over an additive white Gaussian noise (AWGN) model as in (Choukroun & Wolf, 2022; 2024). Bits are modulated as  $x_s = 1 - 2x \in \{-1, +1\}^n$  and transmitted over the AWGN channel with output  $y = x_s + z$ , where  $z \sim \mathcal{N}(0, \sigma^2 I)$ . Decoding aims to recover  $x$  from  $y$ , and performance is evaluated in terms of bit error rate (BER) versus  $E_b/N_0$ .

### 2.2. Transformer-based ECC Decoders

Transformer architectures have been applied to the problem of ECC decoding. ECCT incorporates transformer inference into the decoding process by operat-

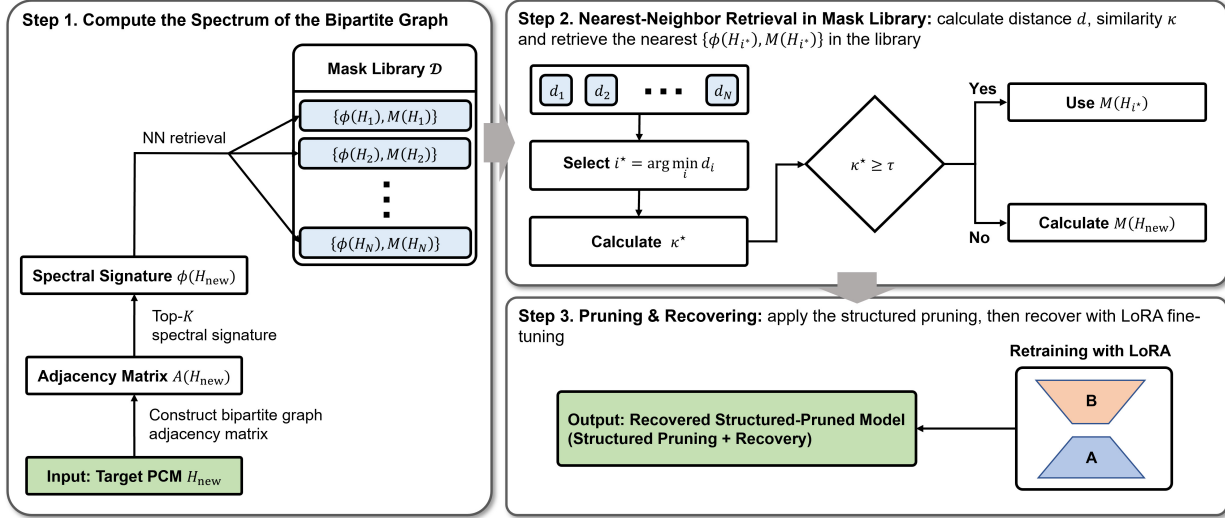


Figure 1. Proposed SAP framework.

ing on a codeword-invariant input representation and injecting code structure through PCM-derived masked self-attention (Choukroun & Wolf, 2022). FECCT extends this paradigm to a single universal decoder by sharing model parameters across multiple code families and block lengths, while modulating attention based on distances in the bipartite graph. In FECCT, decoding performance is typically recovered through retraining, which involves updating the full set of model parameters (Choukroun & Wolf, 2024). Despite their flexibility, attention heads and FFN blocks in transformer-based ECC decoders incur substantial computational cost and model memory footprint, necessitating efficiency improvements.

Several recent works address these computational and memory bottlenecks by redesigning attention architectures to better exploit code structure (Park et al., 2025), as well as by adopting weight quantization to reduce model footprint (Levy et al., 2024). In contrast to architectural redesigns or quantization-based approaches, we investigate *structured pruning* for transformer-based ECC decoders, removing attention heads and FFN channels to reduce computational cost and model memory footprint while preserving universal decoding capability.

### 2.3. Structured Pruning of Transformers

We build on post-training structured pruning methods for transformers, which remove coarse-grained structural units such as attention heads and FFN channels to obtain practical kernel-level speedups. A pruning mask specifies which units are retained or removed under a given compute budget and can be derived using a range of importance criteria, including magnitude- or activation-based heuristics, gradient- or Taylor-based approximations, and second-

order sensitivity estimates (e.g., Fisher- or Hessian-based scores) computed on a small calibration set (Zafir et al., 2021; Kwon et al., 2022; Cheng et al., 2024). In our work, we adopt a Fisher-based importance estimator (Kwon et al., 2022) as an effective primitive for deriving structured pruning masks from transformer-based ECC decoders.

## 3. SAP: Spectral-Aligned Pruning

Figure 1 provides an overview of the proposed SAP framework. Since deriving a structured pruning mask via code-conditioned importance estimation is costly to repeat for each new code, SAP amortizes this overhead by maintaining a library of previously derived code-mask pairs and reusing a stored mask when the target code is sufficiently similar in terms of its spectral signature. Specifically, SAP computes a spectral signature for  $H_{\text{new}}$  (Section 3.1), performs nearest-neighbor retrieval followed by a threshold-based reuse decision (Section 3.2), and then applies structured head/FFN pruning with a subsequent parameter-efficient recovery step (Section 3.3).

### 3.1. Bipartite Graph Spectrum

SAP requires a unified, structure-aware similarity measure between codes to decide whether a previously computed structured pruning mask can be effectively reused. To motivate this need, we first derive a dedicated structured pruning mask per code from the same pretrained FECCT model (Choukroun & Wolf, 2024). To quantify the similarity between pruning masks, we measure mask overlap using the Jaccard similarity. For two binary structured pruning masks  $M_A$  and  $M_B$ , the Jaccard similarity is defined

Table 1. Cross-code Jaccard similarity between structured pruning masks. Pruning masks are derived on a shared pretrained FECCT backbone using code-conditioned importance estimation (Kwon et al., 2022) with a fixed 40 % pruning ratio.

Code $A$	Code $B$	$J(M_A, M_B)$
BCH (63, 45)	Polar (64, 48)	0.274
BCH (63, 45)	LDPC (49, 24)	0.329
Polar (64, 48)	LDPC (49, 24)	0.187
BCH (63, 45)	BCH (63, 36)	0.711
Polar (128, 64)	Polar (128, 86)	0.663
LDPC (49, 24)	LDPC (121, 70)	0.695
LDPC (121, 70)	LDPC (121, 80)	0.807

as

$$J(M_A, M_B) = \frac{|M_A \cap M_B|}{|M_A \cup M_B|}. \quad (1)$$

As shown in Table 1, the mask overlap measured by the Jaccard similarity varies widely across code pairs even under an identical pruning ratio of 40 %: codes with similar structural properties tend to yield similar masks, whereas structurally dissimilar codes produce markedly different masks. This behavior is consistent with the design of transformer-based ECC decoders, where the parity-check matrix (PCM) constrains attention through the code’s bipartite graph representation (Choukroun & Wolf, 2024). Therefore, it is natural to compare codes at the level of their bipartite graphs. We adopt a spectrum-based similarity criterion: the spectrum of the bipartite graph provides a compact summary of graph structure that can be compared across different  $(n, k)$  (Wilson & Zhu, 2008). This spectral representation serves as the similarity descriptor throughout SAP.

Given  $H \in \{0, 1\}^{(n-k) \times n}$ , we construct the bipartite adjacency matrix induced by  $H$ :

$$A(H) = \begin{bmatrix} 0 & H^\top \\ H & 0 \end{bmatrix} \in \{0, 1\}^{(2n-k) \times (2n-k)}. \quad (2)$$

Here, the zero diagonal blocks arise from the bipartite structure, since edges exist only between variable and check nodes. Let  $\lambda_1, \dots, \lambda_{2n-k}$  denote the eigenvalues of the symmetric matrix  $A(H)$ , ordered by decreasing magnitude,  $|\lambda_1| \geq \dots \geq |\lambda_{2n-k}|$ . We define a fixed-dimensional spectral signature by retaining the top- $K$  eigenvalues:

$$\phi(H) = [\lambda_1, \lambda_2, \dots, \lambda_K] \in \mathbb{R}^K, \quad (3)$$

where  $K$  is a hyperparameter. We retain only the top- $K$  eigenvalues to obtain a fixed-dimensional signature comparable across different  $(n, k)$ , following the common use of top- $K$  selection to focus on the most informative spectral components.

For two codes with PCMs  $H_A$  and  $H_B$ , we define the spectral distance as

$$d(\phi(H_A), \phi(H_B)) = \|\phi(H_A) - \phi(H_B)\|_2. \quad (4)$$

### Algorithm 1 Spectral-Aligned Pruning Mask Selection

```

Input: Target PCM  $H_{\text{new}}$ , pruning mask library  $\mathcal{D} = \{(\phi(H_i), M(H_i))\}_{i=1}^N$ , signature length  $K$ , similarity threshold  $\tau$ , scaling parameter  $\beta$ 
Compute spectral signature  $\phi(H_{\text{new}}) \in \mathbb{R}^K$ 
for  $i = 1$  to  $N$  do
     $d_i \leftarrow d(\phi(H_{\text{new}}), \phi(H_i))$ 
end for
     $i^* \leftarrow \arg \min_i d_i$ ,  $d^* \leftarrow \min_i d_i$ 
     $\kappa^* \leftarrow \exp(-\beta d^*)$ 
    if  $\kappa^* \geq \tau$  then
         $\widehat{M}(H_{\text{new}}) \leftarrow M(H_{i^*})$ 
    else
        Compute a new code-specific mask  $M(H_{\text{new}})$ 
         $\widehat{M}(H_{\text{new}}) \leftarrow M(H_{\text{new}})$ 
         $\mathcal{D} \leftarrow \mathcal{D} \cup \{(\phi(H_{\text{new}}), M(H_{\text{new}}))\}$ 
    end if
Output: Selected mask  $\widehat{M}(H_{\text{new}})$ ; updated library  $\mathcal{D}$ 

```

The corresponding spectral similarity score is then defined as follows:

$$\kappa(H_A, H_B) = \exp(-\beta d(\phi(H_A), \phi(H_B))) \in (0, 1], \quad (5)$$

where  $\beta > 0$  is a fixed scaling parameter. This similarity serves as the core retrieval signal in SAP.

### 3.2. Pruning Mask Library and Spectral Retrieval

SAP maintains a pruning mask library to enable mask reuse and avoid repeated pruning mask derivation across different codes. For each code, the library stores the spectral signature of its bipartite graph and the corresponding structured pruning mask for the pretrained FECCT.

Given a code specified by  $H$ , the library stores an entry

$$\mathcal{D}(H) = (\phi(H), M(H)), \quad (6)$$

where  $\phi(H) \in \mathbb{R}^K$  is the spectral signature defined in (3), and  $M(H)$  denotes the structured pruning mask given by

$$M(H) = \left\{ \left( m_{\text{head}}^{(\ell)}(H), m_{\text{FFN}}^{(\ell)}(H) \right) \right\}_{\ell=1}^L. \quad (7)$$

Here,  $m_{\text{head}}^{(\ell)}(H)$  and  $m_{\text{FFN}}^{(\ell)}(H)$  denote the binary mask vectors corresponding to the attention heads and FFN channels in the  $\ell$ -th layer, respectively. For each mask, an element value of 0 indicates that the corresponding attention head or FFN channel is pruned, while a value of 1 indicates that it is retained. When the dependence on  $H$  is clear from context, we omit it for notational simplicity.

We initialize the library with  $N$  reference codes, storing their spectral signatures  $\phi(H)$  and pruning masks

Table 2. Efficiency summary under structured pruning (40 % FLOPs-based ratio). We report FLOPs and parameter counts for the full FECCT and the structurally pruned backbone (after physically removing pruned attention heads and FFN channels), along with the *per-code* LoRA adapter size. FLOPs reduction (Red.) (%) is computed as  $100 \times (\text{Full} - \text{Pruned})/\text{Full}$ .

Codes	FLOPs			Parameters			
	Full (M)	Pruned (M)	Red. (%)	Full (M)	Pruned (M)	LoRA (M)	Ratio (LoRA / Full)
BCH (31, 16)	115.03	69.00	40.00	1.22	0.73	0.090	7.38%
BCH (63, 45)	211.26	126.74	40.00	1.22	0.72	0.089	7.30%
LDPC (96, 64)	403.44	242.05	40.00	1.22	0.70	0.088	7.21%
LDPC (121, 70)	510.39	306.20	40.00	1.22	0.68	0.087	7.13%
Polar (64, 32)	254.80	152.86	40.00	1.22	0.70	0.089	7.39%
Polar (128, 64)	566.23	339.74	40.00	1.22	0.67	0.086	7.05%

$M(H)$  derived from the pretrained FECCT, i.e.,  $\{\mathcal{D}(H_i) = (\phi(H_i), M(H_i))\}_{i=1}^N$ . Given a target code specified by  $H_{\text{new}}$ , we compute  $\phi(H_{\text{new}})$  using (3). We then identify the nearest reference code based on the spectral similarity score defined in (5) as follows:

$$\begin{aligned} i^* &= \arg \min_{i \in \{1, \dots, N\}} d(\phi(H_{\text{new}}), \phi(H_i)), \\ \kappa^* &= \exp(-\beta d(\phi(H_{\text{new}}), \phi(H_{i^*}))). \end{aligned} \quad (8)$$

Based on the spectral similarity score  $\kappa^*$ , SAP applies the following threshold-based reuse rule:

$$\widehat{M}(H_{\text{new}}) = \begin{cases} M(H_{i^*}), & \text{if } \kappa^* \geq \tau, \\ M(H_{\text{new}}), & \text{otherwise,} \end{cases} \quad (9)$$

where  $\tau$  is a similarity threshold. Here,  $M(H_{i^*})$  denotes the pruning mask retrieved from the library, whereas  $M(H_{\text{new}})$  denotes a newly computed code-specific pruning mask obtained via the code-conditioned importance estimation procedure. Specifically, if  $\kappa^* \geq \tau$ , SAP reuses the retrieved pruning mask  $M(H_{i^*})$ ; otherwise, SAP derives a new code-specific mask and updates the library by inserting the new entry:

$$\mathcal{D} \leftarrow \mathcal{D} \cup \{(\phi(H_{\text{new}}), M(H_{\text{new}}))\} \quad (10)$$

This mechanism restricts mask reuse to spectrally aligned codes while progressively incorporating codes that are dissimilar to existing entries into the library. Algorithm 1 summarizes this overall procedure.

### 3.3. Parameter-Efficient Retraining

To recover decoding performance degraded by structured pruning without maintaining a separately retrained model for each code, we perform per-code recovery using *LoRA adapters* on top of the pruned backbone (Hu et al., 2022; Zimmer et al., 2023). Specifically, we freeze the pruned backbone and train only small, code-specific LoRA parameters, which are stored per-code for adaptation. This design substantially reduces the memory overhead compared to saving a fully retrained model for each code. We train these

adapters using the binary cross-entropy (BCE) loss, optionally augmented with a lightweight knowledge distillation (KD) from the pretrained (unpruned) FECCT, following prior work on pruning with distillation (Muralidharan et al., 2024).

For a received sample  $y \in \mathbb{R}^n$ , let  $f_{\theta_t}(y), f_{\theta_s}(y) \in \mathbb{R}^n$  be the outputs of the teacher (unpruned) and student (pruned) models, respectively. We convert the logits into bitwise posterior probabilities via

$$\begin{aligned} q_{t,j} &= \sigma(\text{sign}(y_j) f_{\theta_t}(y)_j), \\ q_{s,j} &= \sigma(\text{sign}(y_j) f_{\theta_s}(y)_j), \end{aligned} \quad (11)$$

and define the KD loss as the average Kullback-Leibler (KL) divergence between bitwise posteriors. The overall recovery objective is

$$\mathcal{L} = \mathcal{L}_{\text{BCE}} + \gamma \mathcal{L}_{\text{KD}}, \quad (12)$$

where  $\gamma$  is a weighting hyperparameter.

We implement this recovery by training LoRA adapters on top of the pruned backbone while keeping all backbone parameters frozen (Hu et al., 2022). For a weight matrix  $W \in \mathbb{R}^{d_{\text{out}} \times d_{\text{in}}}$ , LoRA parameterizes a low-rank update as

$$W' = W + \Delta W, \quad \Delta W = BA, \quad (13)$$

where  $A \in \mathbb{R}^{r \times d_{\text{in}}}$  and  $B \in \mathbb{R}^{d_{\text{out}} \times r}$  with rank  $r \ll \min(d_{\text{in}}, d_{\text{out}})$ . Recovery optimizes only the adapter parameters under the objective in (12). After retraining, the adapters can be merged into the corresponding weights.

Because recovery updates only low-rank adapters, SAP maintains a small set of shared pruned backbone and stores only compact, code-specific LoRA parameters. This substantially reduces per-code storage compared to keeping a separate fully retrained model for each code, while restoring pruning-induced decoding performance degradation in practice.

## 4. Experiments

In this section, we evaluate the proposed *SAP* framework on FECCT, as it supports a unified transformer decoder ar-

Table 3. Decoding performance at  $E_b/N_0 \in \{4, 5, 6\}$  dB. Entries are  $-\ln(\text{BER})$  (higher is better) as in (Choukroun & Wolf, 2022; 2024). Parentheses indicate the performance gap  $\Delta = \text{SAP} - \text{Dedicated}$ . Positive values of  $\Delta$  indicate cases where the SAP mask slightly outperforms the dedicated pruning mask. **Bold values indicate negligible degradation** ( $\Delta \geq -0.15$ ), meaning that SAP achieves performance comparable to dedicated pruning.

Library Ref. Codes	Target Codes	Dedicated Masks			SAP Masks		
		4 dB	5 dB	6 dB	4 dB	5 dB	6 dB
BCH (31, 16)	BCH (31, 11)	4.83	6.37	8.53	4.84 (+0.01)	6.37 (+0.00)	8.47 (-0.06)
	BCH (31, 21)	6.19	8.36	11.20	6.20 (+0.01)	8.26 (-0.10)	11.20 (+0.00)
BCH (63, 51)	BCH (63, 36)	4.53	6.30	8.92	4.51 (-0.02)	6.30 (+0.00)	9.00 (+0.08)
	BCH (63, 45)	5.16	7.33	10.32	5.18 (+0.02)	7.30 (-0.03)	10.16 (-0.16)
LDPC (96, 64)	LDPC (64, 48)	7.40	10.07	13.27	7.40 (+0.00)	10.04 (-0.03)	13.36 (+0.09)
	LDPC (96, 72)	7.31	10.32	13.85	7.33 (+0.02)	10.23 (-0.09)	13.72 (-0.13)
LDPC (121, 60)	LDPC (49, 24)	6.16	8.83	12.67	6.15 (-0.01)	8.80 (-0.03)	12.69 (+0.02)
	LDPC (121, 70)	6.43	10.20	15.80	6.43 (+0.00)	10.12 (-0.08)	15.65 (-0.15)
Polar (64, 48)	Polar (64, 32)	6.10	8.37	11.52	6.16 (+0.06)	8.35 (-0.02)	11.48 (-0.04)
	Polar (64, 43)	6.50	8.96	11.64	6.48 (-0.02)	8.90 (-0.06)	11.66 (+0.02)
Polar (128, 86)	Polar (128, 64)	5.21	7.48	10.61	5.20 (-0.01)	7.47 (-0.01)	10.47 (-0.14)
	Polar (128, 96)	6.04	8.75	12.06	6.02 (-0.02)	8.72 (-0.03)	12.26 (+0.20)

chitecture with a consistent parameter set across multiple code families, block lengths, and rates, which aligns with the design assumptions of SAP.

**Pretraining.** The FECCT backbone is pretrained on BCH, LDPC, and polar codes, using the 12 codes summarized in Appendix C. Pretraining is conducted on the all-zero codewords for 4,000 epochs with a batch size of 256, where  $E_b/N_0$  is uniformly sampled between 2 dB and 7 dB. We use the Adam optimizer and a cosine learning-rate schedule, decaying from  $1 \times 10^{-4}$  to  $1 \times 10^{-6}$ .

**SAP library.** We construct a pruning mask library using six representative ECCs commonly adopted in ECCT-based decoder evaluations, selected to span diverse code families and parameters: BCH (31, 16) and (63, 51), LDPC (96, 64) and (121, 60), and polar (64, 48) and (128, 86) codes (Choukroun & Wolf, 2022; 2024). For the spectral signature in (3), we set  $K = 20$ . We use  $\beta = 0.1$  as the scaling parameter in the spectral similarity score (Appendix D) and empirically set the reuse threshold to  $\tau = 0.5$ .

**Retraining.** For a target code, we perform LoRA-based recovery after structured pruning with rank  $r = 8$  and scaling factor  $\alpha = 16$ . LoRA adapters are applied to all attention projection matrices ( $W_Q$ ,  $W_K$ ,  $W_V$ , and  $W_O$ ) in the transformer. The pruned model is retrained for 100 epochs using both the BCE loss and the KD loss, with the unpruned model as the teacher; in this case, we set  $\gamma = 1$  in (12).

#### 4.1. Efficiency Gains: FLOPs and Parameter Counts

We evaluate the efficiency benefits of our approach along three dimensions: computational cost (FLOPs), the param-

eter count of the shared backbone after structured pruning, and the additional *per-code* parameters required for LoRA-based recovery. Unless otherwise stated, we use a 40 % pruning ratio as the default pruning ratio for the efficiency measurements.

Table 2 shows that structured pruning yields consistent efficiency gains in FLOPs and memory footprint across all evaluated codes. Since we apply a fixed FLOPs-based pruning ratio of 40 % (Kwon et al., 2022), the FLOPs reduction is 40 % for every code by design. Moreover, physically removing pruned attention heads and FFN channels correspondingly reduces the parameter footprint of the shared backbone. To support many codes without storing a fully retrained model for each one, we adopt LoRA and store only compact, per-code adaptation parameters on top of a shared pruned backbone. Table 2 quantifies the resulting storage overhead: the per-code LoRA parameters account for only 7 % to 7.4 % of the full FECCT parameter count. This design enables storage-efficient multi-code deployment by sharing a single backbone while storing only a small set of code-specific parameters for each target code. Importantly, these efficiency gains are achieved without sacrificing decoding performance, as explained in the following section.

#### 4.2. Decoding Performance

We evaluate SAP on various BCH, LDPC, and polar codes by comparing the following decoder configurations: (i) an unpruned retraining baseline, in which the pretrained FECCT is fully fine-tuned for the same number of epochs as the recovery stage; (ii) a dedicated pruned model followed by LoRA recovery; (iii) a SAP model followed by

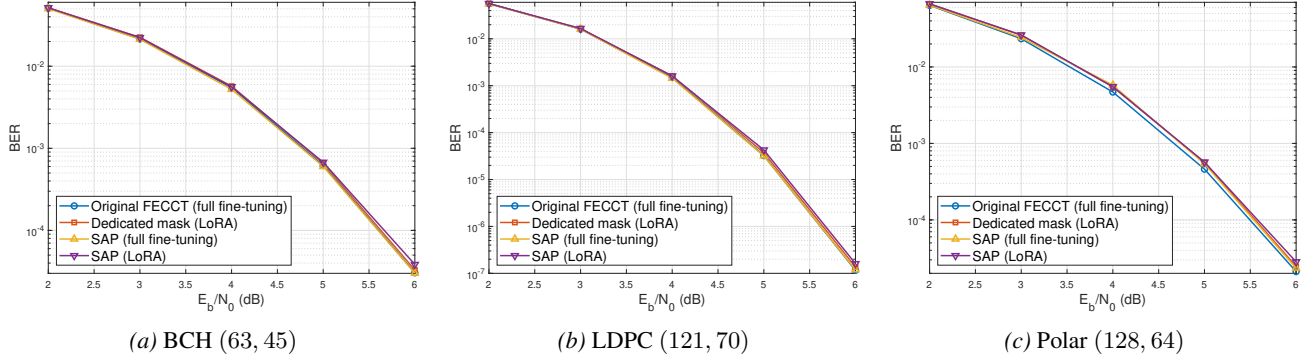


Figure 2. Decoded BER comparison of the pretrained FECCT baseline, the dedicated pruned models, and the SAP models.

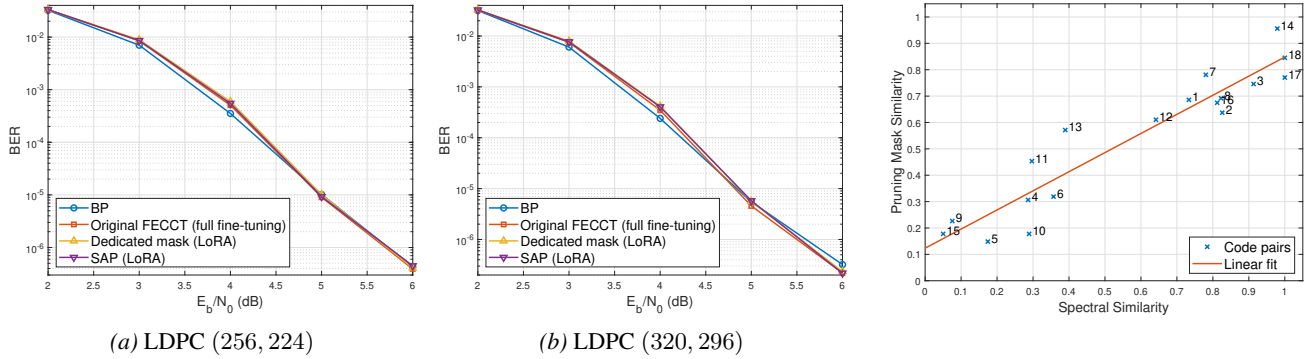


Figure 3. Decoded BER on 5G NR LDPC codes. We compare BP with 50 iterations, dedicated per-code pruning with recovery, and SAP mask reuse with recovery. For both targets, SAP retrieves LDPC (96, 64) as the nearest library entry and reuses its structured pruning mask, achieving performance comparable to dedicated pruning.

full fine-tuning; and (iv) a SAP model followed by LoRA-based recovery. Unless otherwise stated, all pruned models use the same pruning ratio and recovery budget. Accordingly, our evaluation considers two factors: pruning strategy (dedicated vs. SAP-selected) and recovery method (full fine-tuning vs. LoRA).

Table 3 compares the decoding performance of dedicated and SAP masks across BCH, LDPC, and polar codes at  $E_b/N_0 \in \{4, 5, 6\}$  dB. Performance is reported in terms of  $-\ln(\text{BER})$  as in (Choukroun & Wolf, 2022; 2024), together with the performance gap  $\Delta$ . Across all code families and SNRs, the performance gap  $\Delta$  remains close to zero, with the vast majority of entries satisfying  $\Delta \geq -0.15$ . Positive values of  $\Delta$  indicate cases where the SAP-selected pruning mask slightly outperforms the dedicated pruning mask. This indicates that SAP-selected shared pruning masks achieve decoding performance comparable to code-specific dedicated pruning masks, despite avoiding per-target pruning mask derivation. This behavior is observed across different block lengths and rates within each code family in our evaluation. For completeness, the corresponding results for the original (unpruned) FECCT with

full fine-tuning are reported in Appendix G.

Figure 2 compares BER curves for the evaluated decoder variants. For BCH (63, 45), LDPC (121, 70), and polar (128, 64), the dedicated and SAP curves closely track the unpruned retraining baseline, indicating that structured pruning preserves the decoding performance. Moreover, the SAP (LoRA) curve closely matches that of SAP (full fine-tuning), suggesting that code-specific recovery can be effectively achieved via parameter-efficient adaptation on top of the shared pruned backbone. Additional details on the LoRA hyperparameters are provided in Appendix B. Taken together, these results show that spectrum-guided pruning mask reuse enables structured pruning for FECCT decoders without material accuracy loss: SAP matches dedicated per-code pruning after recovery, and the recovered pruned models closely track the unpruned retraining baseline under the same training schedule. We also observe the same qualitative trends under other pruning ratios (see Appendix H). We further report complementary evaluations on frame error rate (FER), also referred to as block error rate (BLER) (see Appendix E).

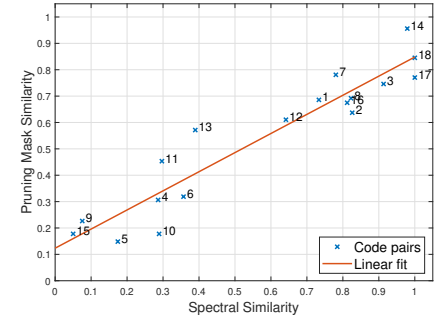


Figure 4. Spectral similarity vs. pruning mask similarity (Jaccard index). Pearson correlation:  $\rho = 0.94$ .

### 4.3. 5G NR LDPC Codes

To evaluate SAP on practical standardized codes, we conduct experiments on 5G NR LDPC codes. For each target code, SAP performs spectral retrieval over the library and selects LDPC (96, 64) as the nearest neighbor, with similarities  $\kappa^* = 0.7793$  for LDPC (256, 224) and  $\kappa^* = 0.7295$  for LDPC (320, 296). We reuse the structured pruning mask of LDPC (96, 64) and apply the same recovery procedure as in the main experiments.

Figure 3 compares the standard belief propagation (BP) decoder, the unpruned retraining baseline of FECCT, and pruned FECCT decoders after recovery using dedicated and SAP-selected masks. Across both code settings, the SAP curves closely track those of the dedicated pruning over the tested  $E_b/N_0$  range, indicating that the proposed SAP is effective for 5G NR LDPC codes. Moreover, compared to BP, the unpruned retraining baseline and the recovered pruned decoders (dedicated and SAP) achieve comparable decoded BER. Overall, these results show that SAP provides effective pruning mask reuse for 5G NR LDPC codes with longer block lengths without sacrificing decoding performance.

## 5. Analysis

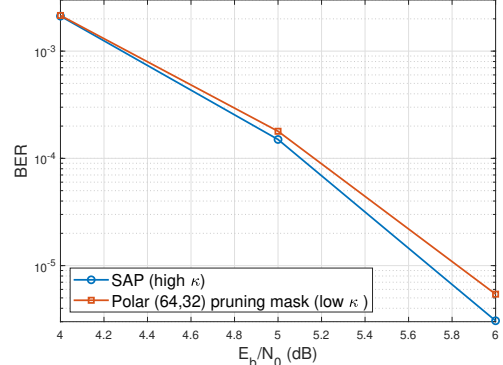
### 5.1. Spectral Similarity Tracks Mask Overlap

Figure 4 illustrates how spectral similarity (5) between bipartite graphs predicts pruning mask similarity. The pruning mask similarity is measured using the Jaccard similarity between structured pruning masks. For readability, we annotate each point with an index, and the corresponding list of code pairs is provided in Appendix A.

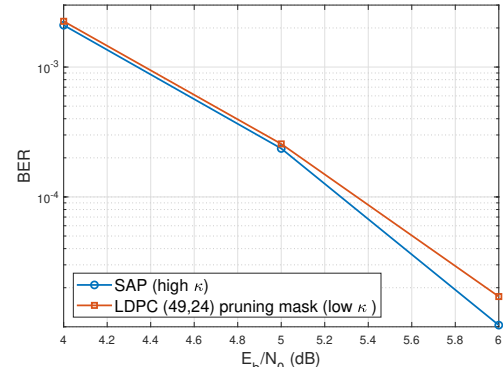
The results reveal a strong positive relationship: code pairs with higher spectral similarity tend to yield more similar pruning masks. A linear fit captures this trend well, with a Pearson correlation coefficient of  $\rho = 0.94$ , indicating a tight alignment between spectral similarity and pruning mask overlap. This empirical result supports the design of SAP, showing that the bipartite graph spectrum serves as a compact and scalable criterion for identifying which previously computed pruning mask is likely to be compatible with a new code. We additionally evaluate alternative structural similarity measures (see Appendix D). The proposed spectral similarity provides the most consistent alignment with pruning mask overlap among the evaluated similarity measures.

### 5.2. Pruning Mask Reuse Fails Under Low Spectral Similarity

This section examines the failure of naive pruning mask reuse when code structures are highly mismatched. We con-



(a) LDPC (49, 24)



(b) Polar (64, 32)

Figure 5. Pruning mask reuse under low spectral similarity ( $\kappa = 0.1456$ ). Reusing a pruning mask derived from a spectrally dissimilar code (LDPC (49, 24) and polar (64, 32)) degrades BER performance relative to SAP’s library-selected mask.

sider two codes from different families, LDPC (49, 24) and polar (64, 32) codes, which exhibit low spectral similarity ( $\kappa = 0.1456$ ). To isolate the effect of pruning mask selection, we conduct a cross-transfer experiment in which each target code is pruned using the other code’s structured pruning mask under the same FLOPs budget, followed by the same recovery procedure used in SAP.

As shown in Figure 5, reusing a pruning mask from a spectrally dissimilar code consistently degrades decoding performance compared to the SAP-selected mask, even after recovery. Since both the pruning ratio and the recovery procedure are held fixed, the observed performance loss is directly attributable to the mismatch between the pruning mask and the target code’s bipartite graph structure. These results indicate that structured pruning masks in FECCT are not universally reusable across codes with low spectral similarity. Selecting a graph-aligned pruning mask is therefore crucial for preserving decoding performance, and SAP’s spectrum-based criterion provides a principled and effective mechanism for mask reuse across structurally diverse codes.

## 6. Conclusion

We presented SAP, a structure-aware pruning framework for universal transformer-based ECC decoders. SAP reduces per-code pruning overhead by enabling pruning mask reuse across spectrally similar codes. Extensive evaluations on BCH, LDPC, and polar codes show that spectral similarity strongly correlates with pruning mask overlap, validating SAP’s threshold-based reuse decision and on-demand library expansion. By combining a shared pruned backbone with parameter-efficient LoRA-based recovery, SAP achieves decoding performance comparable to dedicated per-code pruning while substantially reducing computational cost and model memory footprint. Future work includes integrating SAP with complementary efficiency techniques such as quantization and architecture-level sparsification.

## Impact Statement

This paper presents work whose goal is to advance the field of machine learning by improving the efficiency of transformer-based error-correcting code decoders via structured pruning and spectrum-guided mask reuse. There are many potential societal consequences of our work, none which we feel must be specifically highlighted here.

## References

Cheng, H., Zhang, M., and Shi, J. Q. A survey on deep neural network pruning: Taxonomy, comparison, analysis, and recommendations. *IEEE Transactions on Pattern Analysis and Machine Intelligence*, 46:10558–10578, 2024.

Choukroun, Y. and Wolf, L. Error correction code transformer. In *Advances in Neural Information Processing Systems (NeurIPS)*, volume 35, pp. 38695–38705, 2022.

Choukroun, Y. and Wolf, L. A foundation model for error correction codes. In *International Conference on Learning Representations (ICLR)*, 2024.

Hu, E. J., Shen, Y., Wallis, P., Allen-Zhu, Z., Li, Y., Wang, S., Wang, L., and Chen, W. LoRA: Low-rank adaptation of large language models. In *International Conference on Learning Representations (ICLR)*, 2022.

Kwon, W., Kim, S., Mahoney, M. W., Hassoun, J., Keutzer, K., and Gholami, A. A fast post-training pruning framework for transformers. In *Advances in Neural Information Processing Systems (NeurIPS)*, volume 35, pp. 24101–24116, 2022.

Levy, M., Choukroun, Y., and Wolf, L. Accelerating error correction code transformers. *arXiv preprint arXiv:2410.05911*, 2024.

MacWilliams, F. J. and Sloane, N. J. A. *The Theory of Error-Correcting Codes*. North-Holland, Amsterdam, The Netherlands, 1977.

Michel, P., Levy, O., and Neubig, G. Are sixteen heads really better than one? In *Advances in Neural Information Processing Systems (NeurIPS)*, volume 32, 2019.

Muralidharan, S., Sreenivas, S. T., Joshi, R., Chochowski, M., Patwary, M., Shoeybi, M., Catanzaro, B., Kautz, J., and Molchanov, P. Compact language models via pruning and knowledge distillation. In *Advances in Neural Information Processing Systems (NeurIPS)*, volume 37, pp. 41076–41102, 2024.

Park, S.-J., Kwak, H.-Y., Kim, S.-H., Kim, Y., and No, J.-S. CrossMPT: Cross-attention message-passing transformer for error correcting codes. In *International Conference on Learning Representations (ICLR)*, 2025.

Richardson, T. J. and Urbanke, R. *Modern coding theory*. Cambridge Univ. Press, 2008.

Vaswani, A., Shazeer, N., Parmar, N., Uszkoreit, J., Jones, L., Gomez, A. N., Kaiser, Ł., and Polosukhin, I. Attention is all you need. In *Advances in Neural Information Processing Systems (NeurIPS)*, volume 30, pp. 5998–6008, 2017.

Voita, E., Talbot, D., Moiseev, F., Sennrich, R., and Titov, I. Analyzing multi-head self-attention: Specialized heads do the heavy lifting, the rest can be pruned. In *Proceedings of the Annual Meeting of the Association for Computational Linguistics (ACL)*, pp. 5797–5808, 2019.

Wills, P. and Meyer, F. G. Metrics for graph comparison: A practitioner’s guide. *PLOS ONE*, 15:1–54, 2020.

Wilson, R. C. and Zhu, P. A study of graph spectra for comparing graphs and trees. *Pattern Recognition*, 41: 2833–2841, 2008.

Zafrir, O., Larey, A., Boudoukh, G., Shen, H., and Wasserblat, M. Prune once for all: Sparse pre-trained language models. *arXiv preprint arXiv:2111.05754*, 2021.

Zimmer, M., Andoni, M., Spiegel, C., and Pokutta, S. PERP: Rethinking the prune-retrain paradigm in the era of LLMs. *arXiv preprint arXiv:2312.15230*, 2023.

## A. Code-Pair Indices for Figure 4

Table 4. Code-pair indices used in Figure 4.

Index	Code pair
1	LDPC (49, 24) vs. LDPC (121, 80)
2	LDPC (121, 60) vs. LDPC (121, 80)
3	LDPC (121, 60) vs. LDPC (121, 70)
4	BCH (63, 36) vs. LDPC (49, 24)
5	Polar (64, 32) vs. LDPC (49, 24)
6	BCH (63, 36) vs. LDPC (121, 80)
7	BCH (63, 36) vs. BCH (63, 51)
8	BCH (63, 45) vs. BCH (63, 51)
9	BCH (63, 36) vs. Polar (128, 64)
10	Polar (64, 48) vs. LDPC (121, 80)
11	Polar (64, 48) vs. Polar (128, 64)
12	Polar (64, 32) vs. Polar (64, 48)
13	Polar (64, 48) vs. Polar (128, 86)
14	LDPC (128, 64) vs. LDPC (128, 64) (different random seeds)
15	LDPC (49, 24) vs. LDPC (49, 24) (RREF)
16	BCH (63, 45) vs. BCH (63, 45) (RREF)
17	LDPC (49, 24) vs. LDPC (49, 24) (permutation)
18	BCH (63, 45) vs. BCH (63, 45) (permutation)

For readability, Figure 4 annotates each scatter point with a numeric index rather than a full code-pair label. Table 4 lists the corresponding code pairs. In addition, we use simple linear transformations of the PCM to probe whether pruning mask transferability is governed by *code equivalence* or by the *bipartite graph structure*. Let  $H \in \{0, 1\}^{(n-k) \times n}$  denote a PCM over GF(2).

**RREF (row operations).** We compute the reduced row echelon form (RREF) of  $H$  via Gaussian elimination over GF(2), yielding  $\tilde{H}$ . Since elementary row operations preserve the row space, for any codeword  $x$ ,  $Hx^\top = 0 \pmod{2}$  holds if and only if  $\tilde{H}x^\top = 0 \pmod{2}$ . Thus,  $H$  and  $\tilde{H}$  define the same linear code, while potentially inducing substantially different sparsity and local connectivity patterns in the bipartite graph.

**Column permutation (variable re-indexing).** We also consider a column-permuted PCM  $H' = H\Pi$ , where  $\Pi$  is a permutation matrix. This operation corresponds to re-indexing variable nodes (bit positions), preserving the code up to coordinate permutation and inducing a Tanner graph that is isomorphic up to node relabeling.

These controlled variants (indices 15-18 in Table 4) are introduced to separately examine the effects of code and graph to pruning masks. These help decouple the influence of algebraic code equivalence from bipartite graph structure when interpreting mask overlap and transferability.

## B. LoRA Rank Sensitivity: Recovery Performance vs. Adaptation Cost

Table 5 studies how the LoRA rank  $r$  trades off recovery quality against adaptation cost. As expected, increasing  $r$  increases the number of trainable parameters approximately linearly. For polar (64, 32), moving from  $r = 4$  to 8 roughly doubles trainable parameters (44.3k  $\rightarrow$  88.2k) and yields a clear recovery gain, whereas increasing to  $r = 16$  again doubles the parameters (88.2k  $\rightarrow$  177.4k) but provides only marginal improvement. A similar diminishing-return trend is observed for LDPC (121, 70):  $r = 4 \rightarrow 8$  improves recovery with a near-doubling of parameters (43.5k  $\rightarrow$  87.2k), while  $r = 8 \rightarrow 16$  (87.2k  $\rightarrow$  173.9k) yields comparatively smaller gains. Based on this diminishing-return behavior, we use  $r = 8$  as the default recovery configuration, as it achieves near-saturated recovery performance with substantially fewer trainable parameters than higher-rank settings.

## C. Pretraining Code Set

Table 6 lists the 12 codes used to pretrain the FECCT backbone, covering three representative ECC families (BCH, LDPC, and polar). Following common practice in transformer-based ECC decoder (ECCT/FECCT) evaluations, we select repre-

Table 5. Effect of the LoRA rank  $r$  on post-pruning recovery. We report the number of trainable parameters and  $-\ln(\text{BER})$  at  $E_b/N_0 \in \{4, 5, 6\}$  dB (higher is better).

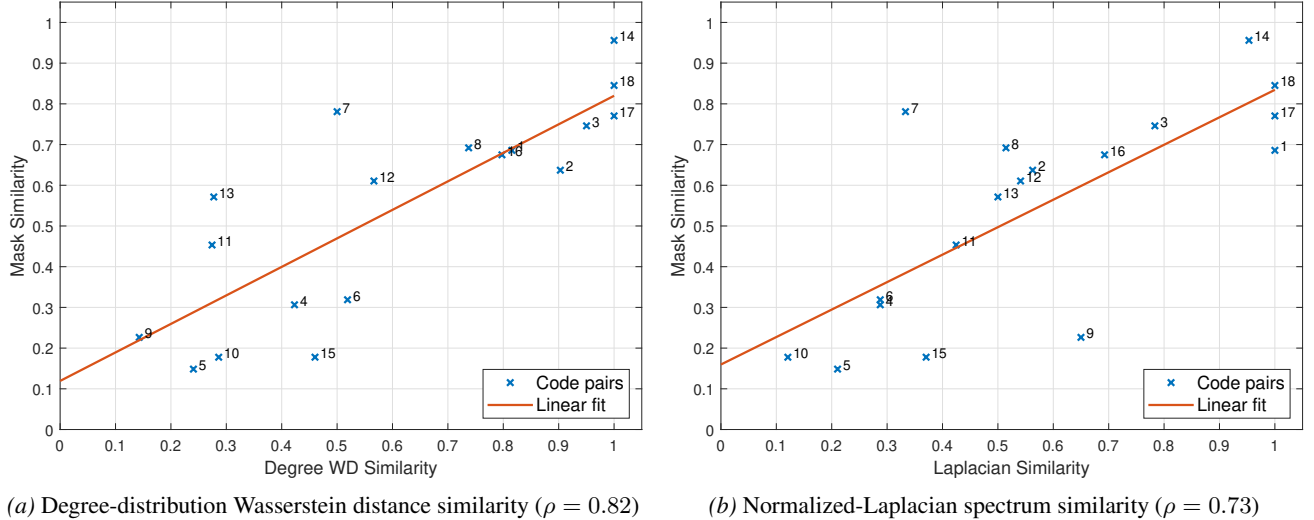
Code	LoRA $r$	Trainable	4 dB	5 dB	6 dB
Polar (64, 32)	4	44,340	5.98	8.11	10.68
	8	88,200	6.16	8.35	11.30
	16	177,360	6.21	8.49	11.34
LDPC (121, 70)	4	43,468	6.38	10.06	15.38
	8	87,176	6.43	10.12	15.64
	16	173,872	6.45	10.32	15.76

Table 6. Pretraining code set for the FECCT backbone.

Family	Codes used for pretraining
BCH	(31, 16), (63, 36), (63, 45), (63, 51)
Polar	(64, 32), (64, 48), (128, 64), (128, 86)
LDPC	(49, 24), (121, 60), (121, 70), (121, 80)

sentative codes spanning a range of rates and block lengths within each family (Choukroun & Wolf, 2022; 2024). This set is used throughout our experiments unless stated otherwise

## D. Alternative Similarity Metrics: Why Adjacency Spectrum is Preferred



(a) Degree-distribution Wasserstein distance similarity ( $\rho = 0.82$ ) (b) Normalized-Laplacian spectrum similarity ( $\rho = 0.73$ )

Figure 6. Correlation between pruning-mask similarity (Jaccard index) and alternative similarity metrics. Each point corresponds to a code pair (indexed as in Table 4), and the red line is a least-squares linear fit. Both metrics exhibit positive correlation with mask similarity, but their correlations are weaker than the adjacency spectrum similarity used by SAP in the main text, supporting the use of adjacency-spectral retrieval.

We consider two alternative graph-based similarity metrics and evaluate how well each predicts pruning-mask similarity. Figure 6 reports Pearson correlations of  $\rho = 0.82$  for degree-distribution Wasserstein distance similarity and  $\rho = 0.73$  for the normalized Laplacian similarity, both of which are lower than the  $\rho = 0.94$  achieved by the adjacency-spectrum similarity adopted in SAP.

**Degree-distribution Wasserstein Distance (WD) similarity.** Given a parity-check matrix  $H$ , we construct its Tanner graph and compute the edge-perspective degree distributions (Richardson & Urbanke, 2008). For two codes, we measure the discrepancy between degree distributions using the 1D Wasserstein distance  $d_{\text{WD}}$ , and convert it into an similarity as

follows:

$$\kappa_{\text{WD}} = \exp(-\beta d_{\text{WD}}). \quad (14)$$

Degree statistics capture only first-order connectivity and are not a complete graph invariant: distinct Tanner graphs can share identical degree distributions. Therefore, degree-based matching can fail to reflect higher-order structural differences beyond degrees, which helps explain its weaker correlation with pruning-mask overlap.

**Normalized-Laplacian spectral similarity.** For each Tanner graph, we form the normalized Laplacian  $L = I - D^{-1/2}AD^{-1/2}$  and compute the spectral signature  $\phi_{\text{Lap}}(H)$  utilizing the smallest  $K$  eigenvalues of  $L$  (ordered  $\lambda_1 \leq \lambda_2 \leq \dots$ ) (Wills & Meyer, 2020). Then, similar to the adjacency-spectrum metric, we define the Laplacian spectral distance:

$$d_{\text{Lap}}(\phi_{\text{Lap}}(H_A), \phi_{\text{Lap}}(H_B)) = \|\phi_{\text{Lap}}(H_A) - \phi_{\text{Lap}}(H_B)\|_2. \quad (15)$$

The corresponding similarity score is then defined using the exponential kernel:

$$\kappa_{\text{Lap}} = \exp(-\beta d_{\text{Lap}}). \quad (16)$$

Compared to adjacency spectra, the normalized Laplacian explicitly normalizes by node degrees through  $D^{-1/2}(\cdot)D^{-1/2}$ , which suppresses degree-scale information. Consequently, by dampening these degree-dependent magnitude signals, the normalized Laplacian discards intensity information that can be critical for identifying the structural units preserved by the pruning masks.

**Median-based calibration of  $\beta$ .** To facilitate a fair comparison across metrics with different native scales, we adopt a uniform, data-driven heuristic to set the decay parameter  $\beta$ . Given a collection of pairwise distances  $d$  (either  $d_{\text{WD}}$  or  $d_{\text{Lap}}$ ), we exclude zero distances (which typically arise from trivial matches) and compute the median  $m = \text{median}(d)$ . We then choose  $\beta$  such that the similarity at the median distance equals 0.5:

$$\exp(-\beta m) = 0.5 \quad \Rightarrow \quad \beta = \frac{\ln 2}{m}. \quad (17)$$

While this calibration is an empirical choice, it serves to center the similarity distribution and prevent saturation near 0 or 1. This ensures that the dynamic range of the similarity scores is consistent across different metrics, allowing for a reliable assessment of their correlation with mask overlap.

## E. Frame Error Rate (FER): Frame-Level Reliability under SAP

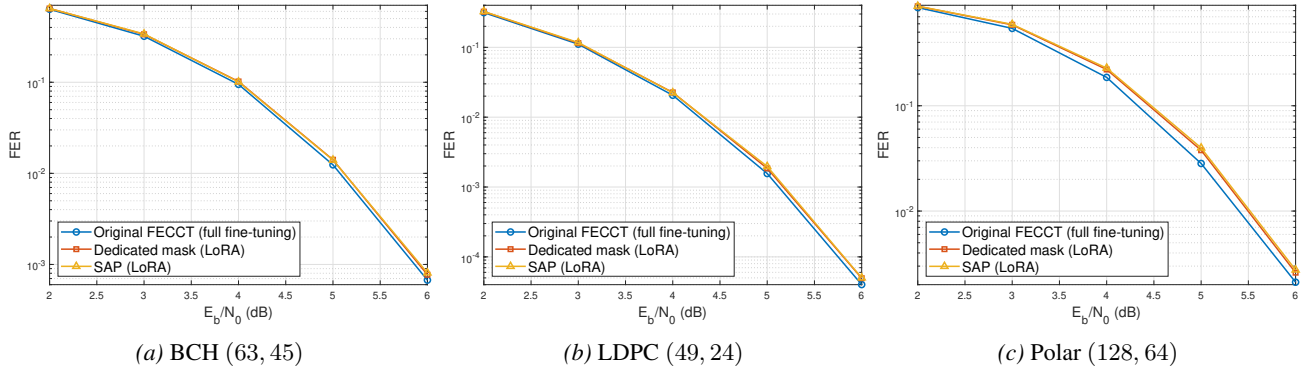


Figure 7. FER comparison of the pretrained FECCT baseline and the pruned decoders after recovery: dedicated per-code pruning vs. SAP mask reuse. Across both codes, SAP closely tracks the dedicated-pruning curve over the tested  $E_b/N_0$  range, suggesting that spectrum-guided mask reuse preserves frame-level reliability.

While the main text focuses on BER, we additionally report FER to evaluate frame-level reliability. As shown in Figure 7, the SAP-reused mask achieves FER comparable to dedicated per-code pruning after recovery for BCH (63, 45), LDPC (49, 24) and polar (128, 64) codes. This indicates that spectrum-guided mask reuse maintains reliability not only at the bit level (BER) but also at the frame level (FER).

Table 7. Impact of the KD loss during recovery on two representative codes. We report  $-\ln(\text{BER})$  at  $E_b/N_0 \in \{4, 5, 6\}$  dB (larger is better). BCE + KD uses the default setting ( $\gamma = 1$ ) with the unpruned model as teacher, whereas BCE disables KD ( $\gamma = 0$ ) and optimizes only the BCE term.

Code	Recovery setting	4 dB	5 dB	6 dB
LDPC (121, 70)	BCE + KD ( $\gamma = 1$ )	6.43	10.06	15.64
	BCE ( $\gamma = 0$ )	6.37	10.04	15.48
Polar (64, 32)	BCE + KD ( $\gamma = 1$ )	6.16	8.35	11.30
	BCE ( $\gamma = 0$ )	6.11	8.24	11.19

## F. Effect of Knowledge Distillation During Recovery

Table 7 indicates that disabling KD leads to a small but consistent degradation in recovery performance under the same retraining budget. Across both codes and all evaluated SNRs, using both the BCE loss and the KD loss improves BER compared to using BCE loss alone. These results support using KD as an auxiliary signal for short post-pruning recovery when a reliable teacher (the unpruned model) is available.

## G. Full Fine-Tuning Results of the Original (Unpruned) FECCT

For completeness, Figure 8 shows the full fine-tuning results of the original (unpruned) FECCT on the codes listed in Table 3. After full fine-tuning, across most codes, the unpruned FECCT yields only a marginal SNR gain relative to pruned models, typically within  $\leq 0.1$  dB over the tested  $E_b/N_0$  range.

## H. Pruning-Ratio Sensitivity

Figure 9 reports BER curves under several pruning ratios for three representative codes, BCH (63, 45), LDPC (49, 24), and polar (128, 64) codes. In the main experiments, we adopt a pruning ratio of 40 % across code families to ensure a consistent efficiency target. We observe that the maximum tolerable pruning ratio can be code-dependent: some codes admit more aggressive structured pruning with minimal degradation, whereas others show earlier performance loss as the pruning ratio increases. For this reason, we adopt 40 % as a conservative default that remains broadly stable across the evaluated code families, while still providing meaningful efficiency gains.

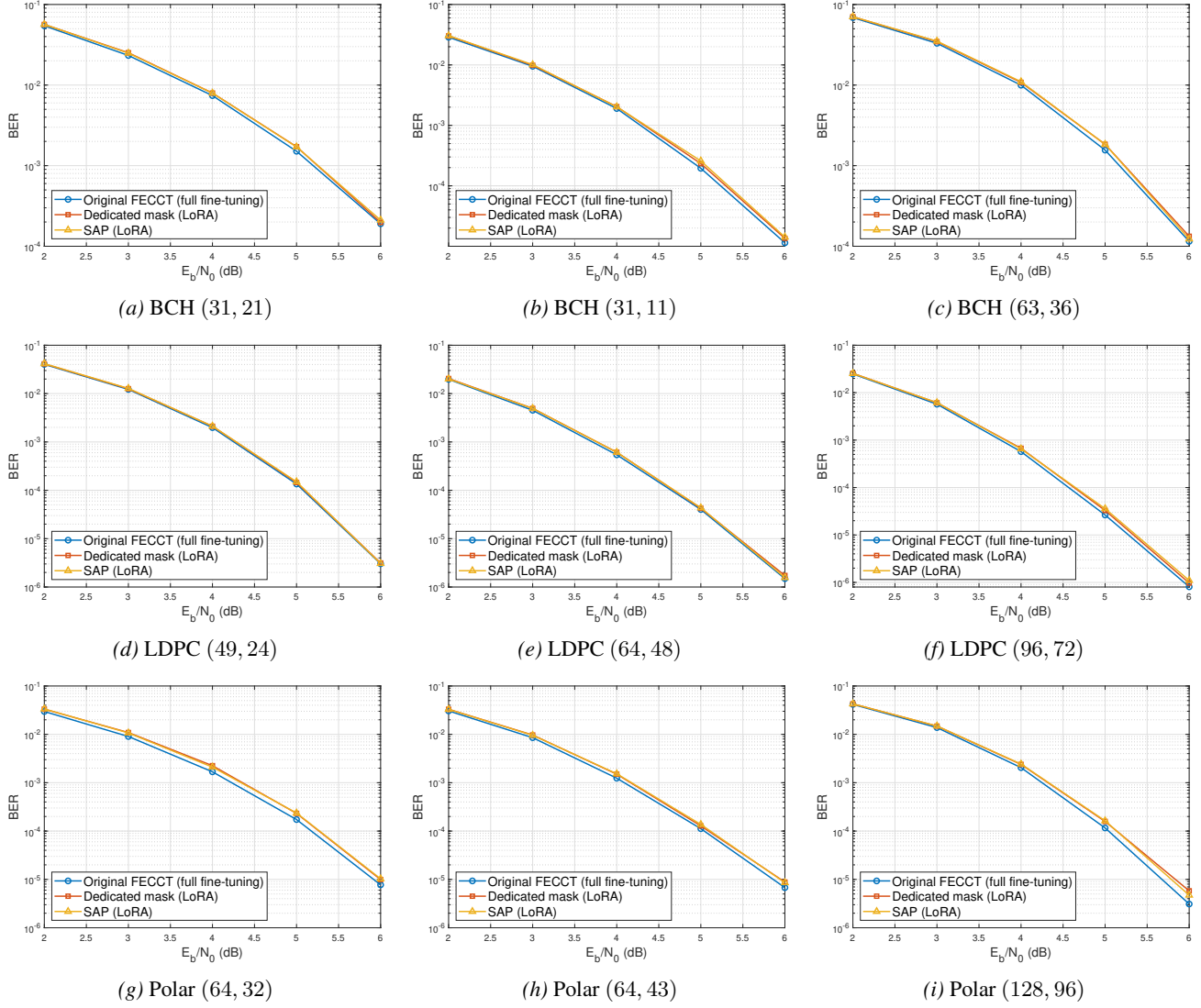


Figure 8. Decoded BER comparison of the pretrained FECCT baseline, the dedicated pruned model, and the SAP model. Results are shown for the codes listed in Table 3.

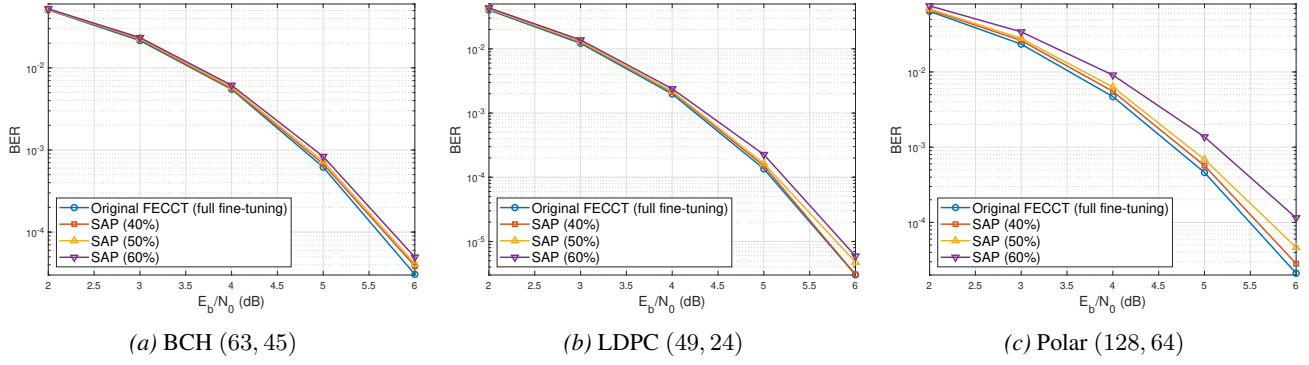


Figure 9. Decoded BER under varying pruning ratios.